

Published in final edited form as:

Glycoconj J. 2014 February ; 31(2): 117–131. doi:10.1007/s10719-013-9505-7.

Protein O-glycosylation in *Lactobacillus buchneri*

Julia Anzengruber,

Department of NanoBiotechnology, NanoGlycobiology unit, Universität für Bodenkultur Wien, Muthgasse 11, 1190 Vienna, Austria, julia.anzengruber@boku.ac.at

Martin Pabst,

Department of Chemistry, Universität für Bodenkultur Wien, Muthgasse 18, 1190 Vienna, Austria, martin.pabst@org.chem.ethz.ch

Laura Neumann,

Department of Chemistry, Universität für Bodenkultur Wien, Muthgasse 18, 1190 Vienna, Austria, laura.neumann@boku.ac.at

Gerhard Sekot,

Department of NanoBiotechnology, NanoGlycobiology unit, Universität für Bodenkultur Wien, Muthgasse 11, 1190 Vienna, Austria, gerhard.sekot@acib.at

Stefan Heini,

Christian Doppler Laboratory for Genetically Engineered Lactic Acid Bacteria, Department of Biotechnology, Universität für Bodenkultur Wien, Muthgasse 11, 1190 Vienna, Austria, setfan.heini@boku.ac.at

Reingard Grabherr,

Christian Doppler Laboratory for Genetically Engineered Lactic Acid Bacteria, Department of Biotechnology, Universität für Bodenkultur Wien, Muthgasse 11, 1190 Vienna, Austria, reingard.grabherr@boku.ac.at

Friedrich Altmann,

Department of Chemistry, Universität für Bodenkultur Wien, Muthgasse 18, 1190 Vienna, Austria, fierdich.altmann@boku.ac.at

Paul Messner, and

Department of NanoBiotechnology, NanoGlycobiology unit, Universität für Bodenkultur Wien, Muthgasse 11, 1190 Vienna, Austria, paul.messner@boku.ac.at

Christina Schäffer

Department of NanoBiotechnology, NanoGlycobiology unit, Universität für Bodenkultur Wien, Muthgasse 11, 1190 Vienna, Austria

Abstract

© Springer Science+Business Media New York 2013

christina.schaeffer@boku.ac.at

Present Address: M. Pabst, Department of Chemistry and Applied Biosciences, ETH Zurich, Zurich, Switzerland

Present Address: G. Sekot, Austrian Centre of Industrial Biotechnology, Muthgasse 18, 1190 Vienna, Austria

Based on the previous demonstration of surface (S-) layer protein glycosylation in *Lactobacillus buchneri* 41021/251 and because of general advantages of lactic acid bacteria for applied research, protein glycosylation in this bacterial species was investigated in detail. The cell surface of *L. buchneri* CD034 is completely covered with an oblique 2D crystalline array (lattice parameters, $a = 5.9$ nm; $b = 6.2$ nm; $\gamma \sim 77^\circ$) formed by self-assembly of the S-layer protein SlpB. Biochemical and mass spectrometric analyses revealed that SlpB is the most abundant protein and that it is *O*-glycosylated at four serine residues within the sequence S₁₅₂-A-S₁₅₄-S₁₅₅-A-S₁₅₇ with, on average, seven Glc(α 1-6) residues, each. Subcellular fractionation of strain CD034 indicated a sequential order of SlpB export and glycosylation as evidenced by lack of glycosylation of cytosolic SlpB. Protein glycosylation analysis was extended to strain *L. buchneri* NRRL B-30929 where an analogous glycosylation scenario could be detected, with the S-layer glycoprotein SlpN containing an *O*-glycosylation motif identical to that of SlpB. This corroborates previous data on S-layer protein glycosylation of strain 41021/251 and let us propose a species-wide S-layer protein *O*-glycosylation in *L. buchneri* targeted at the sequence motif S-A-S-S-A-S. Search of the *L. buchneri* genomes for the said glycosylation motif revealed one further ORF, encoding the putative glycosyl-hydrolase LbGH25B and LbGH25N in *L. buchneri* CD034 and NRRL B-30929, respectively, for which we have indications of a glycosylation comparable to that of the S-layer proteins. These findings demonstrate the presence of a distinct protein *O*-glycosylation system in Gram-positive and beneficial microbes.

Keywords

Glycobiology; *O*-glycosylation motif; Lactic acid bacteria; Glycosyl-hydrolase; S-layer

Introduction

Glycosylation is one of the most common protein modifications involved in many pivotal biological processes [1]. While having long been overlooked, nowadays, glycosylation of proteins in bacteria is becoming increasingly documented, including both *O*- and *N*-linked protein glycosylation [2–8]. Most bacteria known to glycosylate proteins have specialized glycosylation systems where a few abundant polymeric surface proteins such as flagellins, pilins, or surface (S-) layer proteins [9–11] as well as virulence factors of pathogens [12–14] are glycosylated. Relatively few bacterial species have been shown to have general protein glycosylation systems where glycans are added to many proteins with diverse functions and subcellular localizations. *Campylobacter* spp. were the first bacteria demonstrated to have a general protein glycosylation system where target proteins are *N*-glycosylated [15], with *Campylobacter jejuni* being the first bacterium for which the glycosylation machinery was fully reconstituted in *E. coli* [16]. General *O*-glycosylation systems have so far been described in pathogenic *Neisseria* spp. [17], in the major gut symbiont *Bacteroides fragilis* [18] and in phylogenetically related species, such as the periodontal pathogen *Tannerella forsythia* [19].

In Gram-positive and beneficial bacteria, such as lactic acid bacteria, general glycosylation systems have not been documented so far. Lactic acid bacteria are used in various ways of applied research due to their GRAS (generally regarded as safe) status, including food and

feed production [20] and production of recombinant proteins and metabolites [21–23]. Furthermore, they are promising candidates for carbohydrate engineering purposes, aimed at, for instance, the improvement of the therapeutic behavior of protein drugs [24] or the design of immunomodulatory agents [25].

Glycosylation of lactobacillar proteins was previously reported for the S-layer proteins of *Lactobacillus buchneri* 41021/251 [26], *Lactobacillus helveticus* ATCC12046 [27], *Lactobacillus acidophilus* NCFM [28], *Lactobacillus plantarum* 41021/252 [26], and various *Lactobacillus kefir* strains [29]. These S-layer glycoproteins share the common feature of self-assembling into closed, 2D crystalline arrays on the bacterial cell surface [8, 30]. While S-layer glycosylation of most of these proteins was inferred only from a positive periodic acid-Schiff staining reaction of an SDS-PAGE gel, for *L. buchneri* 41021/251, the S-layer glycans were shown to be glucose oligomers attached to serine residues of the S-layer protein [26]. Other known lactobacillar glycoproteins are extracellular, cell wall-hydrolyzing enzymes containing O-linked carbohydrate moieties, found in *Streptococcus faecium* ATCC 9790 [31], *L. plantarum* WCFS1 [32, 33], and *Lactobacillus rhamnosus* GG [34]. Recently, even cysteine S-glycosylation, a novel post-translational modification, was reported in glycopeptide bacteriocins of *L. plantarum* [35, 36]. The demonstration of glycans on several extracellular proteins of lactobacilli supports recent studies pinpointing the importance of lactobacillar cell surface glycosylation for, e.g. adhesion and biofilm formation [37] as well as gastrointestinal persistence [38] and adaptation [39].

Here, S-layer protein glycosylation in the species *L. buchneri* was investigated in detail. *L. buchneri* strains are Gram-positive, obligatory hetero-fermentative, facultative anaerobes; they have been isolated from different sources, ranging from stable grass silage [40, 41], ethanol production plants [42], pickled juice [43] and acid-coagulating cheese samples [44] to the human intestine [45]. One strain was shown to have probiotic effects manifested in cholesterol reduction, acid and bile tolerance, and antimicrobial activity [43]. *L. buchneri* strains are intensively investigated because of their property of efficient preservation of animal feed silages against aerobic spoilage. The obligatory hetero-fermentative nature and acid resistance have drawn attention to this species for applications as silage starter culture [46–51]. *L. buchneri* strains used in this work include *L. buchneri* CD034, isolated from grass silage [40, 41], *L. buchneri* 41021/251, isolated from a dairy factory [26], and *L. buchneri* NRRL B-30929, isolated from an ethanol production plant [42]. The complete genome sequences of *L. buchneri* CD034 [52] and *L. buchneri* NRRL B-30929 [53] were published recently.

To assess the significance of protein glycosylation in the species *L. buchneri* this study specifically deals with the i) identification and electron-microscopic visualization of the S-layer glycoprotein SlpB of *L. buchneri* CD034, ii) elucidation of its S-layer glycan structure, iii) analysis of SlpB glycosylation sites, iv) determination of the cellular site of SlpB glycosylation, v) identification of the S-layer glycoprotein SlpN in the closely related strain *L. buchneri* NRRL B-30929, and vi) investigation of glycosylation of the putative glycosylhydrolases, *LbGH25B* and *LbGH25N*, in *L. buchneri* CD034 and NRRL B-30929, respectively.

Materials and methods

Bacterial strains and culture conditions

L. buchneri CD034 [40, 41, 52], *L. buchneri* NRRL B-30929 [42, 53, 54], and *L. buchneri* 41021/251 [26] were grown in De Man-Rogosa-Sharpe (MRS) broth (Oxoid, Basingstoke, Hampshire, UK) [55] at 37 °C without shaking. *Escherichia coli* DH5α cells (Life Technologies, Vienna, Austria) and *E. coli* BL21 (DE3) cells (Life Technologies) were cultivated at 37 °C and 200 rpm in Luria-Bertani (LB) medium supplemented with 50 µg mL⁻¹ kanamycin (Km).

Freeze-etching and transmission electron microscopy

Cell morphology of *L. buchneri* CD034 was examined by transmission electron microscopy (TEM) of freeze-etched intact bacteria [56]. Cells were harvested by centrifugation and washed three times with sterile double-distilled water (MilliQ-water). Freeze-etching was carried out in a BAF 060 unit (Leica, Wetzlar, Germany). Fracturing and etching of frozen samples was done at -96 °C for 90 s prior to platinum/carbon shadowing. Replicas were purified for 30 min in 70 % sulfuric acid, neutralized in MilliQ-water and subsequently subjected to 14 % sodium hypochloride solution (for 3-5 min), followed by three washing steps in MilliQ-water water and immobilization on 400-mesh TEM copper grids (Agar Scientific, Stansted, UK). Samples were investigated in a Tecnai G² 20 Twin TEM (FEI, Eindhoven, The Netherlands), operating at 80 keV, and micrographs were taken with an FEI Eagle 4 k CCD camera (4,096×4,096 pixels). S-layer lattice parameters were obtained from the power spectra directly taken in the TEM as published recently [57].

Production and purification of recombinant proteins

The coding sequences for the S-layer protein SlpB of *L. buchneri* CD034 (LBUCD034_1608) devoid of the N-terminal signal peptide sequence (corresponding to amino acids 1–31 of the pre-protein) was PCR-amplified with the primers (Life Technologies) SlpB_F (5'- AATCACCATGGGCAAATCATATGCCAAAGTTAC -3', NcoI site is underlined) and SlpB_R (5'- AATCACTCGAGATTAAACGGTGTAAACAGTAAC -3', XhoI site is underlined), digested with NcoI- and XhoI and ligated into pET28a+ expression vector (Novagen, Madison, WI, USA). Similarly, the coding sequences for *Lb* GH25B (LBUCD034_0240) and *Lb* GH25N (Lbuc_0200) were PCR-amplified without signal peptides (amino acids 1–29) using the primers *Lb*GH25B/N_F (5'- AATCATCTAGAAATAATTTTGTTTAACTTTAAGAAGGAGATATACCATGGCTTTG ACGCCGTCCAGTACC-3', XbaI site is underlined) and *Lb* GH25B/N_His_stop_R (5'- AATCAAAGCTTTTAATGATGATGATGATGATTCAAATAACCGCGCCAAATC C-3', HindIII site is underlined), digested with XbaI and HindIII- and ligated into pET28a+. The resulting recombinant plasmids (pET28a-SlpB_His₆, pET28a-*Lb*GH25B_His₆ and pET28a-*Lb*GH25N_His₆) were propagated in *E. coli* BL21 Star (DE3) for production of hexahistidine-tagged proteins.

The transformed strains were grown in LB broth supplemented with kanamycin (50 µg mL⁻¹) at 37 °C and 200 rpm. At the mid-exponential growth phase (OD₆₀₀~0.6), protein

expression was induced with 1 mM isopropyl β -D-1-thio-galactopyranoside (IPTG) and cultivation was continued for 4 h. Cells were pelleted by centrifugation ($10,000 \times g$, 20 min), resuspended in lysis buffer (50 mM sodium citrate buffer, pH 6.2, 0.1 % Triton X-100) and, after addition of lysozyme ($800 \mu\text{g mL}^{-1}$; Sigma-Aldrich, Vienna, Austria) and benzonase (50 U mL^{-1} ; Sigma-Aldrich), incubated for 30 min at 37 °C. Bacteria were further lysed by ultrasonication (Branson sonifier, duty cycle 50 %; output 6) applying ten cycles of 10 pulses with 30 s breaks, each, and insoluble inclusion bodies containing the recombinant proteins were pelleted. The proteins were extracted from the pellets with binding buffer (50 mM sodium citrate buffer, pH 5.5, 5 M GdHCl (guanidinium hydrochloride), 20 mM imidazol, 0.5 M NaCl) for 1 h at 4 °C. The extracts were subjected to centrifugation and membrane-filtering (0.45- μm pore size). The resulting protein samples were applied to a 1-ml HisTrap HP column (GE Healthcare, Vienna, Austria) and recombinant proteins were recovered with elution buffer (50 mM sodium citrate buffer, pH 5.5, 5 M GdHCl, 1 M imidazol, 0.5 M NaCl). Recombinant proteins were dialyzed against 50 mM sodium citrate buffer, pH 5.5.

SDS-PAGE

SDS-PAGE was carried out on 15 % and 20 % slab gels in a Mini Protean electrophoresis apparatus (Bio-Rad, Vienna, Austria) according to Laemmli [58]. Laemmli buffer contained 62.5 mM Tris-HCl, pH 6.9, 2 % SDS, 1 % β -mercaptoethanol, and 10 % glycerol. Protein bands were visualized with colloidal Coomassie Brilliant Blue R-250 (CBB) staining reagent, carbohydrates with periodic acid-Schiff (PAS) staining reagent or with Pro-Q Emerald 300 fluorescent stain (Life Technologies) [59], and the gels were imaged at 700 nm using the Odyssey imaging system (LICOR, Lincoln, NE, USA) and at 300 nm using the Infinity-3000 apparatus (Vilber-Lourmat, Marne-la-Vallée, France), respectively.

Western-immunoblotting

Immunization of mice and preparation of polyclonal antiserum against purified recombinant SlpB and the predicted glycosyl-hydrolase *LbGH25N* was done at EF-BIO s.r.o. (Bratislava, Slovakia). Due to high amino acid homology (99 %) of the predicted glycosyl-hydrolases, the *LbGH25N*-specific antiserum recognized also the homologous protein *LbGH25B*.

Proteins were transferred from the SDS-PAGE gel to a polyvinylidene difluoride membrane (Bio-Rad) using a Mini Trans-Blot Cell (Bio-Rad). The S-layer and glycosyl-hydrolase specific antisera were used in combination with IR Dye 800CW goat anti-mouse antibody (LI-COR) and detection was performed at 800 nm using the Odyssey Infrared Imaging System (LI-COR).

O-glycan preparation

The S-layer proteins SlpB and SlpN as well as the predicted glycosyl-hydrolases *LbGH25B* and *LbGH25N* of *L. buchneri* CD034 and *L. buchneri* NRRL B-30929, respectively were excised from SDS-PAGE gels and O-glycans were isolated by applying in-gel reductive β -elimination [60]. Excised gel slices were transferred to a 1.5-ml Eppendorf tube, covered with 250–500 μL of 1 M NaBH_4 in 0.5 M NaOH, and incubated at 50 °C for 18 h. Excess of salt was removed using 10 mg HyperSepHypercarb SPE cartridges (Thermo Fisher

Scientific, Vienna, Austria) according to published protocols [61–63]. For comparison, *O*-glycans of the *S*-layer protein *L. buchneri* 41021/251 were isolated by applying in-gel reductive β -elimination with 1 M NaBD₄ in 0.5 M NaOH. Borohydride- and borodeuteride-reduced glycans were vacuum-dried and further analyzed.

Monosaccharide analysis

To identify SlpB glycan constituents, borohydride-reduced *O*-glycans were hydrolyzed with 25 % TFA at 110 °C for 4 h and released monosaccharides were analyzed by high-performance anion-exchange chromatography with pulsed electrochemical detection (HPAEC-PED) (Dionex, Sunnyvale, CA, USA, [64]).

LC-ESI-MS

Borohydride- and borodeuteride-reduced *O*-glycans were analyzed by PGC-ESI-MS as described recently (Hypercarb, 0.32×150 mm, inner diameter 5 μ m) [19, 63, 65]. Ammonium formate buffer (0.3 % formic acid, pH 3.0) was used as buffer A, and a gradient was performed from 0 % to 35 % acetonitrile in buffer A within 35 min using a Dionex Ultimate 3000 (cap flow, 8 μ L min⁻¹). Detection was done by an ESI-Q-TOF Global Ultima from Micromass (Waters, Eschborn, Germany). Data were evaluated using MassLynx 4.0 software.

Proteomics

For the identification of peptides of the *L. buchneri* CD034 and *L. buchneri* NRRL B-30929 glycoproteins, an in-gel trypsin digest of the respective bands from SDS-PAGE gels was performed as described recently [19].

Extracted peptides from *L. buchneri* CD034 were further subjected to RP liquid chromatography coupled to ESI-MS/MS [63]. GPM and the X!tandem algorithm (<http://www.thegpm.org/>) were used for protein database search of the MS/MS data. Results were further evaluated using log(e) values to estimate correctness of peptide assignments.

L. buchneri NRRL B-30929 peptides were dissolved in 50 % acetonitrile and 0.1 % trifluoroacetic acid. An aliquot (0.5 μ l) was directly spotted onto a ground steel sample plate and analyzed by MALDI-TOF MS with α -cyanocinnamic acid as matrix. The sample was analyzed in positive ion mode using a Bruker Autoflex Speed (Bruker Daltonics, Bremen, Germany) equipped with a Smartbeam-II solid-state 1,000 Hz laser; typically 1,000–2,000 shots were summed. Data were analyzed and predicted using the ProteinProspector MS-Fit and MS-Digest on-line software (<http://prospector.ucsf.edu>). SignalP 4.0 Server was used for prediction of signal peptides. Secondary structure prediction of SlpB was computed with PSIPRED protein structure prediction server.

O-glycosylation site analysis

Mass spectrometric determination of the *O*-glycosylation sites was performed according to a published protocol [66]. Briefly, an in-gel trypsin digest of the respective band on SDS-PAGE gels was performed, tryptic peptides were extracted and dried under vacuum. The whole digest was further digested with GluC in 20 mM ammonium bicarbonate overnight

and the digest was further fractionated by RP chromatography (see above). Glyco-positive fractions were evaluated by ESI-MS. Glycans were released from the peptide by ammonia-based non-reductive β -elimination (25 % ammonia for 18 h at 37 °C). The peptide was further subjected to RP liquid chromatography coupled to ESI-MS/MS [63]. The deglycosylated peptide was sequenced and free serine residues could be distinguished from originally glycan-carrying serines by a mass difference of one Da.

Subcellular fractionation of *L. buchneri* CD034

L. buchneri CD034 was grown overnight in MRS broth at 37 °C without shaking. The bacterial cell pellet obtained after centrifugation ($10,000 \times g$, 20 min) was washed with 50 mM Tris-HCl, pH 7.2 (buffer B) and, subsequently, lysed by ultrasonication in buffer B (Branson sonifier, duty cycle 50 %; output 8) by applying six cycles of 10 pulses, with 30 s breaks, each.

Cell wall fraction Cell wall fragments were pelleted ($30,000 \times g$, 15 min) and resuspended in buffer B, containing 1 % Triton X-100, and pelleted again. After four washing steps with buffer B, proteins were resuspended in PBS and mixed with Laemmli buffer prior to SDS-PAGE analysis.

Cytosol Cytosolic proteins were obtained from the supernatant of the centrifugation step directly after ultrasonication during the cell wall isolation described above. Proteins were precipitated with trichloroacetic acid (20 % final concentration) at 4 °C for 30 min. After centrifugation ($9,000 \times g$, 20 min), precipitated proteins were washed twice with ice-cold 100 % acetone. The pellet was air-dried and proteins resuspended in Laemmli buffer.

Results

Description of the cell surface of *L. buchneri* CD034

L. buchneri CD034 possesses a typical Gram-positive cell wall profile with a thick peptidoglycan layer that is additionally covered by an S-layer as outermost cell envelope decoration. This S-layer is formed by self-assembly of the glycoprotein SlpB into a 2D lattice. Freeze-etching experiments of intact bacterial cells showed an oblique S-layer lattice with the base vectors $a = 5.9$ nm, $b = 6.2$ nm, and an enclosed angle of $\gamma \sim 77^\circ$ (Fig. 1). This compares well to the S-layer lattice parameters of *L. buchneri* strains 41021/251 ($a = 5.4$ nm, $b = 6.1$ nm, and $\gamma \sim 80^\circ$) [29] and ATCC 4005 [67]. For the latter strain, careful inspection of the published power spectrum and also of an undisturbed area of the S-layer protein lattice as revealed by a freeze-etched preparation of intact cells, unambiguously revealed the presence of an S-layer with oblique lattice symmetry (center-to-center spacing, ~ 6.0 nm) in contrast to the published hexagonal lattice symmetry.

SDS-PAGE analysis of protein glycosylation in *L. buchneri* CD034

Strong carbohydrate staining reactions with Pro-Q Emerald reagent upon separation of a crude cell extract by SDS-PAGE were observed for *L. buchneri* CD034 (Fig. 2, lane 2). The most abundant glyco-positive stained protein band with an apparent molecular mass of ~ 60 kDa (indicated by an arrow in Fig. 2) was excised from the SDS-PA gel, digested with

trypsin, and subjected to reversed phase LC (RP)-ESI-MS/MS peptide mapping. This glycoprotein could be clearly identified as the S-layer protein of the bacterium by running the MS/MS data against the *L. buchneri* CD034 proteome database using GPM and the X! tandem algorithm (<http://www.thegpm.org/>). The high abundance of that protein on the CBB-stained SDS-PA gel of the whole cellular proteome (Fig. 2, lane 1) correlates with the feature of S-layer proteins being the most abundant cellular proteins, with a total protein biosynthesis effort of up to 20 % being devoted to S-layer protein biosynthesis. The high amount of S-layer proteins is required for a complete coverage of the bacterial cell with a closed S-layer lattice during all stages of the growth cycle [30]. The detected S-layer glycoprotein, SlpB (gene LBUCD034_1608), is one out of eight putative S-layer precursor proteins encoded on the genome of *L. buchneri* CD034 [52]. It is composed of 558 amino acid residues corresponding to a calculated molecular mass of 58.3 kDa and contains 11 % of α -helices, 30 % of β -sheets, and 59 % of random coils according to computed secondary structure prediction; this is in agreement with the predicted secondary structure of other lactobacillar S-layer proteins [68]. As predicted by SignalP 4.0 Server and confirmed by ESI-MS/MS peptide mapping (data not shown), the S-layer protein contains an N-terminal signal peptide of 31 amino acids, exhibiting the sequence MKKSLKKTTFAGVAALS FVAVAGVSSTNASA which includes the commonly found A-X-A motif preceding the cleavage site for type I signal peptidases [69]. Overall SlpB possesses a basic pI of 10.2 that is typical of lactobacillar S-layer proteins [30, 70]. Interestingly, the amino acid sequence of the newly identified S-layer protein SlpB includes the amino acid motif S-S-A-S-S-A-S-S-A, which is also present in the S-layer protein of *L. buchneri* strain 41021/251 [26].

Additionally, a second, ~42-kDa, slightly blurred, glyco-positive band of lower abundance was detected with Pro-Q Emerald reagent (indicated with by asterisk in Fig. 2). Details about this band are given below.

S-layer glycan profiles of *L. buchneri* CD034 and *L. buchneri* 41021/251

The presence of the amino acid signature motif S-S-A-S-S-A-S-S-A, ranging from amino acid 151 to 159 within SlpB of the currently investigated *L. buchneri* CD034 as well as in the *L. buchneri* 41021/251 S-layer protein [26], let us hypothesize that comparable or even identical S-layer protein glycosylation might occur in these bacteria. This hypothesis was tested by first analyzing the S-layer glycan structure of SlpB of *L. buchneri* CD034 and comparing it with the known S-layer glycan structure of strain 41021/251 [26]. Extracts of cellular proteins of either bacterial strain were separated by SDS-PAGE and S-layer protein bands were excised from the 15 % SDS-PA gels. S-layer glycans from *L. buchneri* CD034 were released from the protein backbone by in-gel reductive β -elimination using borohydride, while those of strain 41021/251 were released using borodeuteride. Subsequently, glycan analysis was performed by LC-PGC (porous graphitized carbon)-ESI-MS/MS. The LC profile clearly indicated the presence of identical glycans on the S-layer proteins of *L. buchneri* CD034 and on 41021/251 (Fig. 3a), and showed both glycans to be composed of hexose units and, most probably, according to identical retention times of the S-layer glycans of either strain on the PGC column [65], of Glc(α 1-6). Figure 3b shows a summarized ESI-MS spectrum representing the mass units of repeating hexose units. *L.*

buchneri CD034 S-layer glycans were found with monoisotopic values of 848, 1,010, 1,172 and 1,334 Da corresponding to homooligomers composed of five, six, seven and eight units, respectively. As expected, a mass increase of 1 Da was observed for the borodeuteride-reduced S-layer glycans of strain 41021/251 compared to borohydride-reduced S-layer glycans of strain CD034 (Fig. 3b). Further, monosaccharide analysis of borohydride-reduced and TFA-hydrolyzed S-layer glycans from *L. buchneri* CD034 was performed by HPAEC-PED. The only monosaccharide constituent detected was glucose (Fig. 3c), suggesting that the SlpB glycans consist of a glucose oligomer; this is corroborated by identical PGC retention times of the S-layer glycans of either strain.

Glycosylation sites in the S-layer protein of *L. buchneri* CD034

After an in-gel trypsin digest of the glycosylated S-layer protein SlpB of *L. buchneri* CD034, the glycopeptide (amino acid sequence, 147SASASSASSASSAEQTTALTDAQK₁₇₀) was analyzed by LC-ESI-MS. A major peak in the spectrum at an m/z value of 6828.51 was found to correspond to the sum of the mass of the amino acids and 28 glucose residues (Fig. 4a). The mass accuracy of this peak compared to the calculated m/z value of 6828.57 is -8.79 ppm. The whole tryptic sample was further digested with GluC and the smallest possible glycopeptide was fractionated by RP-HPLC. An aliquot of the vacuum-dried glycopeptide was subjected to ammonia-based non-reductive β -elimination [66]. During that procedure, glycosylated serines were transformed into ammonia-derivatives leading to a mass decrease of 1 Da compared to non-glycosylated serines. The deglycosylated peptide was further analyzed by RP-ESI-TOF-MS/MS (Fig. 5, Table 1). Four serine residues (underlined) within the sequence S-S₁₅₂-A-S₁₅₄-S₁₅₅-A-S₁₅₇-S-A could be detected with the above described mass decrease and, therefore, identified as the glycosylation sites on the S-layer protein SlpB of *L. buchneri* CD034 (compare with Fig. 4a). Distributing 28 glucoses, as found in the major glycopeptide peak, over the four glycosylation sites resulted in an O-glycan consisting of, on average, seven glucose residues. A schematic drawing of the S-layer glycoprotein of *L. buchneri* CD034 including the glycosylation sequence motif and the O-glycan structure is given in Fig. 4b.

Cellular localization of S-layer protein glycosylation in *L. buchneri* CD034

To determine the subcellular localization of the S-layer glycosylation event, (glyco)proteins were isolated from the cell wall and the cytosol, and Western-immunoblotting for S-layer detection as well as PAS staining for glycan detection was performed. While Western-immunoblotting with SlpB-specific antiserum confirmed the presence of the S-layer protein in both the cell wall and the cytosolic fractions, only the cell wall fraction exhibited strong reactivity with the PAS reagent, the cytosolic fraction, in contrast, showed no significant reactivity (Fig. 6). This observation supports our hypothesis of a sequential order of S-layer protein export to the cell surface and glycosylation.

Identical S-layer protein glycosylation among *L. buchneri* strains and determination of a common S-layer glycosylation motif

Based on the detected commonalities of *O*-glycosylation among S-layer proteins in *L. buchneri* CD034 and *L. buchneri* 41021/251, protein glycosylation analysis was extended to strain *L. buchneri* NRRL B-30929 [53] in order to potentially unravel a general S-layer protein glycosylation theme in this bacterial species. *In silico* proteome analysis of *L. buchneri* NRRL B-30929 revealed the presence of two gene products containing an S-S-A-rich region potentially representing a glycosylation motif. These are Lbuc_0578 and Lbuc_1557 containing the amino acid sequences $_{151}\text{S-S-A-S-S-A-S-S-A}_{159}$ and $_{149}\text{S-S-A-S-S-A-S}_{156}$, respectively. Comparable glycoprotein patterns were observed in crude cell extracts of *L. buchneri* strains NRRL B-30929 and CD034 according to SDS-PAGE analysis (Fig. 7a), revealing two glyco-positive protein bands and with apparent molecular masses of ~65 kD and 42 kDa, respectively. The prominent glycoprotein band at ~65 kDa (indicated with an arrow in Fig. 7a, lane 2) was identified as the S-layer protein SlpN (gene Lbuc_1557) of *L. buchneri* NRRL B-30929 after in-gel trypsin digest and MALDI-MS/MS analysis (data not shown). SlpN contains an N-terminal signal peptide including a type I signal peptidase cleavage site and possesses a basic pI of 9.9, which all compares well to SlpB of *L. buchneri* CD034.

For glycan analysis, the band corresponding to glycosylated SlpN was subjected to LC-ESI-MS after in-gel reductive β -elimination. *O*-Glycans, identical to the S-layer glucose homooligomer of strains CD034 and 41021/251 could be identified on the S-layer of *L. buchneri* NRRL B-30929 (Fig. 7b). Based on this observation, the S-S-A-rich sequences of all identified S-layer glycoproteins were aligned revealing the presence of the confirmed glycosylation motif S-A-S-S-A-S of the S-layer protein SlpB of *L. buchneri* CD034 (Fig. 7c).

Indication of a putative glycosyl-hydrolase in *L. buchneri* possessing the S-layer glycosylation theme

Glycans from the ~42-kDa glyco-positive protein band of *L. buchneri* strains CD034 and NRRL B-30929 on SDS-PAGE (indicated with asterisks in Figs. 2 and 7a) were released from the protein backbone by in-gel borohydride-reductive β -elimination and subjected to LC-ESI-MS. Glycan profiles identical to that of the S-layer glycans were detected, showing an oligosaccharide consisting of hexose residues (Fig. 7b).

In silico proteome analysis of *L. buchneri* CD034 and NRRL B-30929 indicated the presence of two further proteins, besides the S-layer proteins, containing the characteristic S-A-S-S-A-S glycosylation motif (Fig. 7c). These are the putative extracellular glycosyl-hydrolase homologues *LbGH25B* (gene LBUCD034_0240) and *LbGH25N* (gene Lbuc_0200) of *L. buchneri* CD034 and NRRL B-30929, respectively, both containing a glycosyl-hydrolase family 25 domain. Similar to the S-layer proteins, the highly homologous putative glycosyl-hydrolases *LbGH25B* and *LbGH25N* contain an N-terminal, 29-amino acid signal peptide including a type I signal peptidase cleavage site and possess a basic pI of 9.5.

Western-immunoblot analysis of crude cell extracts from *L. buchneri* CD034 and *L. buchneri* NRRL B-30929 using glycosyl-hydrolase specific antiserum detected both *LbGH25B* and *LbGH25N* at an apparent molecular mass of ~42 kDa (Fig. 8, lane 1 and 3) which is in accordance with the apparent molecular mass of the additional glyco-positive protein band as inferred from SDS-PA gels (Fig. 8a). Further, purified recombinant, non-glycosylated *LbGH25B* and *LbGH25N* were applied to the immunoblots, revealing a slightly downshifted apparent molecular mass when compared to the native glycosyl-hydrolases (Fig. 8, lanes 2 and 4). These data supported a posttranslational modification of the glycosyl-hydrolases and confirmed the identities of the 42-kDa bands as *LbGH25B* and *LbGH25N*. As evidenced by LC-ESI-MS the modification would be glycans identical to the *O*-glycans attached to the S-layer proteins.

Closer inspection of the SDS-PA gels revealed that the native glycosyl-hydrolases appear as double bands, with the band of lower molecular mass running at the same size as the recombinant enzyme (Fig. 8, lanes 1–4), indicative of the presence of non-glycosylated *LbGH25B* and *LbGH25N* in addition to the glycosylated enzymes in the native *L. buchneri* hosts. The only slight shift in molecular mass between glycosylated (upper band) and non-glycosylated (lower band) glycosyl-hydrolases can be well explained by a difference of only ~1.3 kDa resulting from the 8-unit glucose oligomer. To exclude that matrix effects would cause the different running behavior of the different *LbGH25B* and *LbGH25N* forms, *i.e.*, native, glycosylated *versus* recombinant, non-glycosylated, the recombinant, purified enzymes were mixed with the *L. buchneri* cell extracts prior to application onto the SDS-PA gel. On a Western blot, the double bands of both *LbGH25B* and *LbGH25N* could be still clearly detected by the glycosyl-hydrolase-specific antiserum, with the lower bands now appearing more intensive due to the contribution of the recombinant proteins migrating at the same size (Fig. 8, lane 5 and 6). This supported our assumption that *LbGH25B* and *LbGH25N* are glycoproteins with a certain fraction of the native enzyme being non-glycosylated.

Discussion

We report the presence of an S-layer with oblique lattice symmetry covering *L. buchneri* CD034 cells. We identified the S-layer protein SlpB as most abundant protein of the whole cellular proteome and as the LBUCD034_1608 translation product, one out of eight open reading frames on the genome of *L. buchneri* CD034 encoding putative S-layer proteins [52]. Furthermore, we provided evidence of S-layer protein glycosylation by using a combined biochemical and mass spectrometric approach. It was demonstrated that the S-layer protein of *L. buchneri* CD034 carries *O*-glycans composed of homooligomers of, on average, seven Glc(α 1-6) residues. The glycosylation sites on the SlpB protein were identified as four serines (underlined) within the sequence S-S₁₅₂-A-S₁₅₄-S₁₅₅-A-S₁₅₇-S-A by ammonia-based non-reductive β -elimination combined with ESI-MS/MS.

These results concur with the finding that protein glycosylation in lactobacilli occurs preferentially at domains rich in alanine, serine and also threonine residues (AST domain), as it was shown for the major autolysin Acm2 and hypothesized for several other cell wall associated proteins in *L. plantarum* [32, 33, 71]. A functional role of AST domains,

however, is still unexplored. Bacterial *O*-glycans containing glucose as the only carbohydrate constituent have so far only been documented for our reference strain *L. buchneri* 41021/251 [26] and have been suggested for an *N*-acetylmuramylhydrolase in the lactic acid bacterium *Streptococcus faecium* [31]. Besides that, several protein *O*-glycans were reported in lactobacilli so far, including mannose-containing structures of *L. rhamnosus* [34] and GlcNAc-containing structures of *L. plantarum* [32] as well as other glycans in *L. acidophilus* showing ConA lectin reactivity [28] and in *L. kefir* according to PAS staining [29]. However, none of these glycans has been structurally elucidated.

Concerning the cellular topology of the S-layer protein glycosylation process, our data on the cellular localization of the S-layer glycoprotein of *L. buchneri* CD034 reveal a sequential order between protein export to the cell surface and glycosylation. This corroborates previous observations indicating that (i) the S-layer glycosylation process occurs on the external face of the cytoplasmic membrane [72–74], and (ii) S-layer glycosylation is lagging behind S-layer protein biosynthesis, evidenced by the presence of non-glycosylated SlpB in the cytosol. Similar results concerning the cellular topology of protein glycosylation in lactobacilli were obtained for protein *O*-glycosylation in *L. rhamnosus* GG, where the secreted protein Msp1 was shown to be only glycosylated in the supernatant fraction [34].

We further demonstrated that the discovered S-layer glycosylation theme is also valid for the strain *L. buchneri* NRRL B-30929. The common glycosylation motif S-A-S-S-A-S which is part of the seven amino-acid stretch S-S-A-S-S-A-S was identified within the investigated S-layer protein SlpN of *L. buchneri* NRRL B-30929. Also, S-layer *O*-glucans identical to those attached to SlpB could be identified on SlpN glycoprotein band after separation of a crude cell extract on SDS-PAGE. These findings suggest the presence of species-wide S-layer protein *O*-glycosylation within the sequence motif S-A-S-S-A-S in *L. buchneri* strains.

There are strong indications that the S-layer glycosylation theme can be extended to another *L. buchneri* protein. The putative glycosyl-hydrolases *LbGH25B* and *LbGH25N* of *L. buchneri* CD034 and NRRL B-30929, respectively, were found to be the only proteins in the proteome of either strain, in addition to the S-layer proteins, that contain the characteristic sequence motif S-A-S-S-A-S. Compared to the S-layer proteins, these enzymes are of markedly lower abundance according to CBB- and PAS-stained SDS-PAGE and Western-immunoblotting. The “S-layer” glucose oligomer could be unambiguously detected by mass spectrometry on the corresponding glyco-positive protein band of either *L. buchneri* strain. This, together with the observed migration difference between native and recombinant *LbGH25B* and *LbGH25N* detected with glycosyl-hydrolase-specific antiserum on a Western-immunoblot, supports the posttranslational modification of the glycosyl-hydrolases by glycosylation. The scenario of different proteins of a bacterium carrying the “S-layer glycan” is not new; it has been shown recently for the oral pathogen *Tannerella forsythia* [19]. We would like to note that due to the low abundance of *LbGH25B* and *LbGH25N* in *L. buchneri* cell extracts, a glycoproteomics approach using glycopeptides, as has been performed with the S-layer glycoprotein SlpB, has not been successful, so far. For this purpose, homologous overexpression of the glycosyl-hydrolases is currently under way in our laboratory.

LbGH25B and *LbGH25N*, both, contain a glycosyl-hydrolase family 25 domain, which predicts them to function as bacterial cell wall hydrolases. Several reports on glycosylated extracellular cell wall-hydrolyzing enzymes in lactic acid bacteria are in line with our finding of *LbGH25B* and *LbGH25N* being glycosylated. It is interesting to note that the first example of a proven glycosylated enzyme in bacteria was a glycosyl-hydrolyzing enzyme, namely the endogenous, autolytic *N*-acetylmuramoyl hydrolase of *Streptococcus faecium* [31]. Glycosylation of AcmB, the peptidoglycan-hydrolyzing *N*-acetylglucosaminidase of *Lactococcus lactis*, was proposed based on the presence of potential *O*- and *N*-glycosylation sites [75]. *O*-glycans attached to the N-terminal AST domain were found on the extracellular autolysin Acm2 of *Lactobacillus plantarum* [32] and also *Lactobacillus rhamnosus* expresses *O*-glycosylated Msp1 (major secreted protein), a cell wall hydrolase [34, 76].

The glycosyltransferases involved in the protein glucosylation pathway of *L. buchneri* strains are currently unknown. Especially, *O*-oligosaccharyltransferases (*O* - OTases) as key modules of many glycosylation systems display relatively low homology and typically have rather broad substrate specificities [77, 78] which makes their identification challenging. A high number of transmembrane spanning domains of the putative glycosyl transferases and homologous gene products LBUCD034_2252 and Lbuc_2151 as well as LBUCD034_0503 and Lbuc_0464 of *L. buchneri* CD034 and NRRL B-30929, respectively, make them possible *O*-OST candidates responsible for coupling of the glucose oligomer to specific serine residues on the target proteins. More detailed studies are needed to identify involved enzymes and to obtain a deeper understanding of the protein *O*-glucosylation machinery in *L. buchneri*.

The lactobacillar glycoproteins investigated in this study, *i.e.*, the S-layer proteins SlpB and SlpN as well as the enzymes *LbGH25B* and *LbGH25N*, share common properties; this includes a basic pI, which is a common trait of S-layer proteins of lactobacilli [30, 70], the presence of the S-A-S-S-A-S motif, and a type I signal peptidase cleavage site required for protein export across the cytoplasmic membrane, which supports that these glycoproteins are extracellularly located. Glycosylation of extracellular proteins in *L. buchneri* might possibly facilitate adherence to solid substrates, support cell-cell interaction and contribute as cellular sugar coat to the protection against environmental stresses and proteolytic degradation.

In conclusion, we provided evidence of species wide S-layer *O*-glucosylation in *L. buchneri* strains within a common, serine rich sequence motif and provided strong indications that *L. buchneri* glycosyl-hydrolases undergo the same *O*-glucosylation process. These findings pinpoint new opportunities for glyco-engineering of customized glycans in a Gram-positive, beneficial and safe bacterial organism.

Acknowledgments

We thank Siqing Liu (U.S. Department of Agriculture, Agricultural Research Service, Renewable Product Technology Research Unit, University of Illinois, USA) for kindly providing *L. buchneri* NRRL B-30929, and Andrea Scheberl and Sonja Zayni for excellent technical assistance.

Financial support came from the Austrian Science Fund FWF, projects P21954-B20 (to C.S.) and P24305-B20 (to P.M.), the PhD programme "BioToP - Biomolecular Technology of Proteins" (Austrian Science Fund, FWF project

W1224), the Hochschuljubiläumssstiftung der Stadt Wien, project H-2442/2012 (to J.A.), and the Christian Doppler Laboratory for Genetically Engineered Lactic Acid Bacteria (to R.G.).

Abbreviations

SlpB	S-layer protein of <i>L. buchneri</i> CD034
SlpN	S-layer protein of <i>L. buchneri</i> NRRL B-30929
LbGH25B	Glycosyl-hydrolase of <i>L. buchneri</i> CD034
LbGH25N	Glycosyl-hydrolase of <i>L. buchneri</i> NRRL B-30929

References

- Varki, A.; Cummings, RD.; Esko, JD.; Freeze, HH.; Stanley, P.; Bertozzi, CR.; Hart, GW.; Etzler, ME. Essentials of glycobiology. 2nd edn.. Cold Spring Harbor Laboratory Press; Cold Spring Harbor: 2009. p. 484
- Upreti RK, Kumar M, Shankar V. Bacterial glycoproteins: functions, biosynthesis and applications. Proteomics. 2003; 3:363–379. [PubMed: 12687605]
- Schmidt MA, Riley LW, Benz I. Sweet new world: glycoproteins in bacterial pathogens. Trends Microbiol. 2003; 11:554–561. [PubMed: 14659687]
- Hitchen PG, Dell A. Bacterial glycoproteomics. Microbiology. 2006; 152:1575–1580. [PubMed: 16735721]
- Nothaft H, Szymanski CM. Protein glycosylation in bacteria: sweeter than ever. Nat. Rev. Microbiol. 2010; 8:765–778. [PubMed: 20948550]
- Messner P. Bacterial glycoproteins. Glycoconj. J. 1997; 14:3–11. [PubMed: 9076508]
- Messner P, Sleytr UB. Bacterial surface layer glycoproteins. Glycobiology. 1991; 1:545–551. [PubMed: 1822235]
- Ristl R, Steiner K, Zarschler K, Zayni S, Messner P, Schäffer C. The S-Layer glycome—adding to the sugar coat of bacteria. Int. J. Microbiol. 2011; 2011:127870. [PubMed: 20871840]
- Messner P, Steiner K, Zarschler K, Schäffer C. S-layer nanoglycobiology of bacteria. Carbohydr. Res. 2008; 343:1934–1951. [PubMed: 18336801]
- Hartley MD, Morrison MJ, Aas FE, Børud B, Koomey M, Imperiali B. Biochemical characterization of the O-linked glycosylation pathway in *Neisseria gonorrhoeae* responsible for biosynthesis of protein glycans containing *N, N'*-diacetylglucosamine. Biochemistry. 2011; 50:4936–4948. [PubMed: 21542610]
- Logan SM. Flagellar glycosylation—a new component of the motility repertoire? Microbiology. 2006; 152:1249–1262. [PubMed: 16622043]
- Dobos KM, Swiderek K, Khoo K-H, Brenmann PJ, Belisle JT. Evidence for glycosylation sites on the 45-kilodalton glycoprotein of *Mycobacterium tuberculosis*. Infect. Immun. 1995; 63:2846–2853. [PubMed: 7622204]
- Karlyshev AV, Everest P, Linton D, Cawthraw S, Newell DG, Wren BW. The *Campylobacter jejuni* general glycosylation system is important for attachment to human epithelial cells and in the colonization of chicks. Microbiology. 2004; 150:1957–1964. [PubMed: 15184581]
- Szymanski CM, Wren BW. Protein glycosylation in bacterial mucosal pathogens. Nat. Rev. Microbiol. 2005; 3:225–237. [PubMed: 15738950]
- Szymanski CM, Yao R, Ewing CP, Trust TJ, Guerry P. Evidence for a system of general protein glycosylation in *Campylobacter jejuni*. Mol. Microbiol. 1999; 32:1022–1030. [PubMed: 10361304]
- Wacker M, Linton D, Hitchen PG, Nita-Lazar M, Haslam SM, North JS, Panico M, Morris HR, Dell A, Wren BW, Aebi M. *N*-linked glycosylation in *Campylobacter jejuni* and its functional transfer into *E. coli*. Science. 2002; 298:1790–1793. [PubMed: 12459590]

17. Ku SC, Schulz BL, Power PM, Jennings MP. The pilin *O*-glycosylation pathway of pathogenic *Neisseria* is a general system that glycosylates AniA, an outer membrane nitrite reductase. *Biochem. Biophys. Res. Comm.* 2009; 378:84–89. [PubMed: 19013435]
18. Fletcher CM, Coyne MJ, Villa OF, Chatzidaki-Livanis M, Comstock LE. A general *O*-glycosylation system important to the physiology of a major human intestinal symbiont. *Cell.* 2009; 137:321–331. [PubMed: 19379697]
19. Posch G, Pabst M, Brecker L, Altmann F, Messner P, Schäffer C. Characterization and scope of S-layer protein *O*-glycosylation in *Tannerella forsythia*. *J. Biol. Chem.* 2011; 286:38714–38724. [PubMed: 21911490]
20. Giraffa G, Chanishvili N, Widyastuti Y. Importance of lactobacilli in food and feed biotechnology. *Res. Microbiol.* 2010; 161:480–487. [PubMed: 20302928]
21. Helanto M, Kiviharju K, Leisola M, Nyssölä A. Metabolic engineering of *Lactobacillus plantarum* for production of L-ribulose. *Appl. Environ. Microbiol.* 2007; 73:7083–7091. [PubMed: 17873078]
22. Peterbauer C, Maischberger T, Haltrich D. Food-grade gene expression in lactic acid bacteria. *Biotechnol. J.* 2011; 6:1147–1161. [PubMed: 21858927]
23. Konings WN, Kok J, Kuipers OP, Poolman B. Lactic acid bacteria: the bugs of the new millennium. *Curr. Opin. Microbiol.* 2000; 3:276–282. [PubMed: 10851157]
24. Solá RJ, Griebenow K. Glycosylation of therapeutic proteins. *BioDrugs.* 2010; 24:9–21. [PubMed: 20055529]
25. Wells JM. Immunomodulatory mechanisms of lactobacilli. *Microb. Cell Fact.* 2011; 10:S17. [PubMed: 21995674]
26. Möschl, A.; Schäffer, C.; Sleytr, UB.; Messner, P.; Christian, R.; Schulz, G. Characterization of the S-layer glycoproteins of two lactobacilli. In: Beveridge, TJ.; Koval, SF., editors. *Advances in bacterial paracrystalline surface layers*. Vol. 252. Plenum Press; New York: 1993. p. 281-284.
27. Mozes N, Lortal S. X-ray photoelectron spectroscopy and biochemical analysis of the surface of *Lactobacillus helveticus* ATCC 12046. *Microbiology.* 1995; 141:11–19.
28. Konstantinov SR, Smidt H, de Vos WM, Bruijns SCM, Singh SK, Valence F, Molle D, Lortal S, Altermann E, Klaenhammer TR, van Kooyk Y. S layer protein A of *Lactobacillus acidophilus* NCFM regulates immature dendritic cell and T cell functions. *Proc. Natl. Acad. Sci. U. S. A.* 2008; 105:19474–19479. [PubMed: 19047644]
29. Mobili P, los Ángeles Serradell M, Trejo SA, Avilés Puigvert FX, Abraham AG, Antoni GL. Heterogeneity of S-layer proteins from aggregating and non-aggregating *Lactobacillus kefir* strains. *Antonie van Leeuwenhoek.* 2009; 95:363–372. [PubMed: 19306111]
30. Messner, P.; Schäffer, C.; Egelseer, E.; Sleytr, U. Occurrence, structure, chemistry, genetics, morphogenesis, and functions of S-Layers. In: König, H.; Claus, H.; Varma, A., editors. *Prokaryotic cell wall compounds—structure and biochemistry*. Springer; Berlin: 2010. p. 53-109.
31. Kawamura T, Shockman GD. Purification and some properties of the endogenous, autolytic *N*-acetylmuramoylhydrolase of *Streptococcus faecium*, a bacterial glycoenzyme. *J. Biol. Chem.* 1983; 258:9514–9521. [PubMed: 6874701]
32. Fredriksen L, Mathiesen G, Moen A, Bron PA, Kleerebezem M, Eijsink VGH, Egge-Jacobsen W. The major autolysin Acm2 from *Lactobacillus plantarum* undergoes cytoplasmic *O*-glycosylation. *J. Bacteriol.* 2011; 194:325–333. [PubMed: 22081384]
33. Rolain T, Bernard E, Beaussart A, Degand H, Courtin P, Egge-Jacobsen W, Bron PA, Morsomme P, Kleerebezem M, Chapot-Chartier MP, Dufrene YF, Hols P. *O*-glycosylation as a novel control mechanism of peptidoglycan hydrolase activity. *J. Biol. Chem.* 2013; 288:22233–22247. [PubMed: 23760506]
34. Lebeer S, Claes IJJ, Balog CIA, Schoofs G, Verhoeven TLA, Nys K, von Ossowski I, de Vos WM, Tytgat HLP, Agostinis P, Palva A, Van Damme EJM, Deelder AM, de Keersmaecker SCJ, Wuhrer M, Vanderleyden J. The major secreted protein Msp1/p75 is *O*-glycosylated in *Lactobacillus rhamnosus* GG. *Microb. Cell Fact.* 2012; 11:15. [PubMed: 22297095]
35. Stepper J, Shastri S, Loo TS, Preston JC, Novak P, Man P, Moore CH, Havlí ek V, Patchett ML, Norris GE. Cysteine *S*-glycosylation, a new post-translational modification found in glycopeptide bacteriocins. *FEBS Lett.* 2011; 585:645–650. [PubMed: 21251913]

36. Venugopal H, Edwards PJB, Schwalbe M, Claridge JK, Libich DS, Stepper J, Loo T, Patchett ML, Norris GE, Pascal SM. Structural, dynamic, and chemical characterization of a novel S-glycosylated bacteriocin. *Biochemistry*. 2011; 50:2748–2755. [PubMed: 21395300]
37. Lebeer S, Verhoeven TLA, Francius G, Schoofs G, Lambrichts I, Dufrene Y, Vanderleyden J, De Keersmaecker SCJ. Identification of a gene cluster for the biosynthesis of a long, galactose-rich exopolysaccharide in *Lactobacillus rhamnosus* GG and functional analysis of the priming glycosyltransferase. *Appl. Environ. Microbiol.* 2009; 75:3554–3563. [PubMed: 19346339]
38. Denou E, Pridmore RD, Berger B, Panoff JM, Arigoni F, Brussow H. Identification of genes associated with the long-gut-persistence phenotype of the probiotic *Lactobacillus johnsonii* strain NCC533 using a combination of genomics and transcriptome analysis. *J. Bacteriol.* 2008; 190:3161–3168. [PubMed: 18223069]
39. Marco ML, de Vries MC, Wels M, Molenaar D, Mangell P, Ahrne S, de Vos WM, Vaughan EE, Kleerebezem M. Convergence in probiotic *Lactobacillus* gut-adaptive responses in humans and mice. *ISME J.* 2010; 4:1481–1484. [PubMed: 20505752]
40. Heidl S, Spath K, Egger E, Grabherr R. Sequence analysis and characterization of two cryptic plasmids derived from *Lactobacillus buchneri* CD034. *Plasmid.* 2011; 66:159–168. [PubMed: 21907734]
41. Spath K, Heidl S, Egger E, Grabherr R. *Lactobacillus plantarum* and *Lactobacillus buchneri* as expression systems: evaluation of different origins of replication for the design of suitable shuttle vectors. *Mol. Biotechnol.* 2012; 52:40–48. [PubMed: 22081307]
42. Liu S, Skinner-Nemec KA, Leathers TD. *Lactobacillus buchneri* strain NRRL B-30929 converts a concentrated mixture of xylose and glucose into ethanol and other products. *J. Ind. Microbiol. Biotechnol.* 2008; 35:75–81. [PubMed: 17940817]
43. Zeng XQ, Pan DD, Guo YX. The probiotic properties of *Lactobacillus buchneri* P2. *J. Appl. Microbiol.* 2010; 108:2059–2066. [PubMed: 19912431]
44. Radovanovic RS, Katic V. Influence of lactic acid bacteria isolates on *Staphylococcus aureus* growth in skimmed milk. *Bulg. J. Agric. Sci.* 2009; 15:196–203.
45. Köll P, Mändar R, Smidt I, Hütt P, Truusalu K, Mikelsaar R-H, Shchepetova J, Krogh-Andersen K, Marcotte H, Hammarström L, Mikelsaar M. Screening and evaluation of human intestinal lactobacilli for the development of novel gastrointestinal probiotics. *Curr. Microbiol.* 2010; 61:560–566. [PubMed: 20443005]
46. Danner H, Holzer M, Mayrhuber E, Braun R. Acetic acid increases stability of silage under aerobic conditions. *Appl. Environ. Microbiol.* 2003; 69:562–567. [PubMed: 12514042]
47. Driehuis F, Oude Elferink SJWH, Spoelstra SF. Anaerobic lactic acid degradation during ensilage of whole crop maize inoculated with *Lactobacillus buchneri* inhibits yeast growth and improves aerobic stability. *J. Appl. Microbiol.* 1999; 87:583–594. [PubMed: 10583687]
48. Holzer M, Mayrhuber E, Danner H, Braun R. The role of *Lactobacillus buchneri* in forage preservation. *Trends Biotechnol.* 2003; 21:282–287. [PubMed: 12788549]
49. Kung LJ, Taylor CC, Lynch MP, Neylon JM. The effect of treating alfalfa with *Lactobacillus buchneri* 40788 on silage fermentation, aerobic stability, and nutritive value for lactating dairy cows. *J. Dairy Sci.* 2003; 86:336–343. [PubMed: 12613876]
50. Oude Elferink SJWH, Krooneman J, Gottschal JC, Spoelstra SF, Faber F, Driehuis F. Anaerobic conversion of lactic acid to acetic acid and 1,2-propanediol by *Lactobacillus buchneri*. *Appl. Environ. Microbiol.* 2001; 67:125–132. [PubMed: 11133436]
51. Schmidt RJ, Kung LJ. The effects of *Lactobacillus buchneri* with or without a homolactic bacterium on the fermentation and aerobic stability of corn silages made at different locations. *J. Dairy Sci.* 2010; 93:1616–1624. [PubMed: 20338439]
52. Heidl S, Wibberg D, Eikmeyer F, Szczepanowski R, Blom J, Linke B, Goesmann A, Grabherr R, Schwab H, Pühler A, Schlüter A. Insights into the completely annotated genome of *Lactobacillus buchneri* CD034, a strain isolated from stable grass silage. *J. Biotechnol.* 2012; 161:153–166. [PubMed: 22465289]
53. Liu S, Leathers TD, Copeland A, Chertkov O, Goodwin L, Mills DA. Complete genome sequence of *Lactobacillus buchneri* NRRL B-30929, a novel strain from a commercial ethanol plant. *J. Bacteriol.* 2011; 193:4019–4020. [PubMed: 21622751]

54. Liu S, Bischoff KM, Hughes SR, Leathers TD, Price NP, Qureshi N, Rich JO. Conversion of biomass hydrolysates and other substrates to ethanol and other chemicals by *Lactobacillus buchneri*. *Let. Appl. Microbiol.* 2009; 48:337–342. [PubMed: 19187511]
55. De Man JC, Rogosa M, Sharpe ME. A medium for the cultivation of lactobacilli. *J. Appl. Microbiol.* 1960; 23:130–135.
56. Sleytr UB, Messner P, Pum D. Analysis of crystalline bacterial surface layers by freeze-etching, metal shadowing, negative staining and ultrathin sectioning. *Methods Microbiol.* 1988; 20:29–60.
57. Sekot G, Posch G, Oh Y, Zayni S, Mayer H, Pum D, Messner P, Hinterdorfer P, Schäffer C. Analysis of the cell surface layer ultrastructure of the oral pathogen *Tannerella forsythia*. *Arch. Microbiol.* 2012; 196:525–539. [PubMed: 22273979]
58. Laemmli UK. Cleavage of structural proteins during the assembly of the head of bacteriophage T4. *Nature.* 1970; 227:680–685. [PubMed: 5432063]
59. Hart C, Schulenberg B, Steinberg TH, Leung W-Y, Patton WF. Detection of glycoproteins in polyacrylamide gels and on electroblots using Pro-Q Emerald 488 dye, a fluorescent periodate Schiff-base stain. *Electrophoresis.* 2003; 24:588–598. [PubMed: 12601726]
60. Taylor AM, Holst O, Thomas-Oates J. Mass spectrometric profiling of *O*-linked glycans released directly from glycoproteins in gels using in-gel reductive β -elimination. *Proteomics.* 2006; 6:2936–2946. [PubMed: 16586430]
61. Packer NH, Lawson MA, Jardine DR, Redmond JW. A general approach to desalting oligosaccharides released from glycoproteins. *Glycoconj. J.* 1998; 15:737–747. [PubMed: 9870349]
62. Pabst M, Altmann F. Influence of electrosorption, solvent, temperature, and ion polarity on the performance of LC-ESI-MS using graphitic carbon for acidic oligosaccharides. *Anal. Chem.* 2008; 80:7534–7542. [PubMed: 18778038]
63. Stadlmann J, Pabst M, Kolarich D, Kunert R, Altmann F. Analysis of immunoglobulin glycosylation by LC-ESI-MS of glycopeptides and oligosaccharides. *Proteomics.* 2008; 8:2858–2871. [PubMed: 18655055]
64. Lee Y. High-performance anion-exchange chromatography for carbohydrate analysis. *Anal. Biochem.* 1990; 189:151–162. [PubMed: 2281856]
65. Pabst M, Bondili JS, Stadlmann J, Mach L, Altmann F. Mass + retention time = structure: a strategy for the analysis of *N*-glycans by carbon LC-ESI-MS and its application to fibrin *N*-glycans. *Anal. Chem.* 2007; 79:5051–5057. [PubMed: 17539604]
66. Hanisch, F-G.; Müller, S. The proteomics protocols handbook. Humana Press Inc.; Totowa, New York: 2005. Approaches to the *O*-glycoproteome; p. 439-457.
67. Masuda K, Kawata T. Characterization of a regular array in the wall of *Lactobacillus buchneri* and its reattachment to the other wall components. *J. Gen. Microbiol.* 1981; 124:81–90.
68. Åvall-Jääskeläinen S, Palva A. *Lactobacillus* surface layers and their applications. *FEMS Microbiol. Rev.* 2005; 29:511–529. [PubMed: 15935509]
69. van Roosmalen ML, Geukens N, Jongbloed JDH, Tjalsma H, Dubois J-YF, Bron S, van Dijk JM, Anné J. Type I signal peptidases of Gram-positive bacteria. *Biochim. Biophys. Acta, Mol. Cell Res.* 2004; 1694:279–297.
70. Hynönen U, Palva A. *Lactobacillus* surface layer proteins: structure, function and applications. *Appl. Microbiol. Biotechnol.* 2013; 97:5225–5243. [PubMed: 23677442]
71. Kleerebezem M, Hols P, Bernard E, Rolain T, Zhou M, Siezen RJ, Bron PA. The extracellular biology of the lactobacilli. *FEMS Microbiol. Rev.* 2010; 34:199–230. [PubMed: 20088967]
72. Steiner K, Hanreich A, Kainz B, Hitchen PG, Dell A, Messner P, Schäffer C. Recombinant glycans on an S-layer self-assembly protein: a new dimension for nanopatterned biomaterials. *Small.* 2008; 4:1728–1740. [PubMed: 18816436]
73. Zarschler K, Janesch B, Pabst M, Altmann F, Messner P, Schäffer C. Protein tyrosine *O*-glycosylation—a rather unexplored prokaryotic glycosylation system. *Glycobiology.* 2010; 20:787–798. [PubMed: 20200052]
74. Janesch B, Messner P, Schäffer C. Are the surface layer homology domains essential for cell surface display and glycosylation of the S-layer protein from *Paenibacillus alvei* CCM 2051^T? *J. Bacteriol.* 2012; 195:565–575. [PubMed: 23204458]

75. Huard C, Miranda G, Wessner F, Bolotin A, Hansen J, Foster SJ, Chapot-Chartier M-P. Characterization of AcmB, an *N*-acetylglucosaminidase autolysin from *Lactococcus lactis*. *Microbiology*. 2003; 149:695–705. [PubMed: 12634338]
76. Claes IJJ, Schoofs G, Regulski K, Courtin P, Chapot-Chartier M-P, Rolain T, Hols P, von Ossowski I, Reunanen J, De Vos MD, Palva A, Vanderleyden J, De Keersmaecker SCJ, Lebeer S. Genetic and biochemical characterization of the cell wall hydrolase activity of the major secreted protein of *Lactobacillus rhamnosus* GG. *PLoS One*. 2012; 7:e31588. [PubMed: 22359601]
77. Faridmoayer A, Fentabil MA, Mills DC, Klassen JS, Feldman MF. Functional characterization of bacterial oligosaccharyltransferases involved in *O*-linked protein glycosylation. *J. Bacteriol.* 2007; 189:8088–8098. [PubMed: 17890310]
78. Hug I, Feldman MF. Analogies and homologies in lipopolysaccharide and glycoprotein biosynthesis in bacteria. *Glycobiology*. 2010; 21:138–151. [PubMed: 20871101]

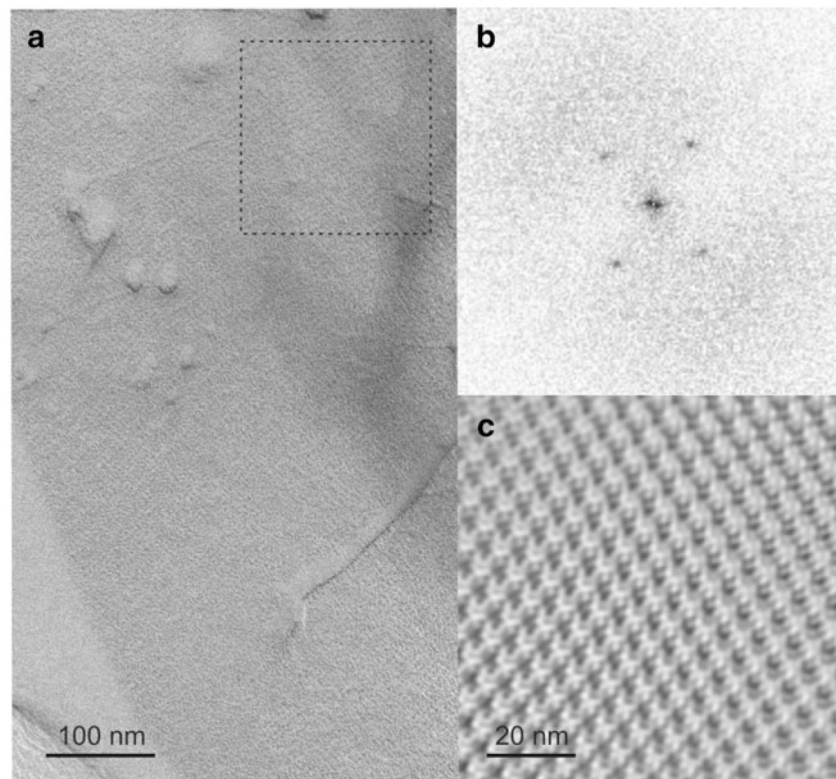


Fig. 1. TEM micrograph of a freeze-etched and metal-carbon-shadowed preparation of *L. buchneri* CD034 cells. **a** Oblique S-layer lattice; **b** power spectrum of the S-layer lattice from the boxed area in **(a)**, **c** lattice reconstruction

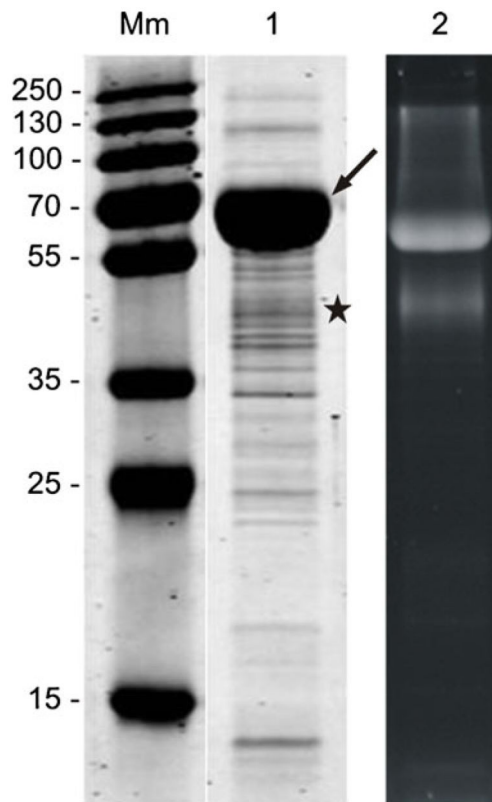


Fig. 2. SDS-PAGE analysis (15 % gel) of a crude cell extract from *L. buchneri* CD034. Mm, PageRuler Plus pre-stained protein ladder (Thermo Scientific). Gels were stained with CBB (lane 1) and Pro-Q Emerald (lane 2). Two glyco-positive protein bands were detected. The arrow indicates the S-layer glycoprotein SlpB of *L. buchneri* CD034 which makes up the main portion of the whole cellular proteome. A second ~42-kDa, glyco-positive protein was detected and is indicated by an asterisk

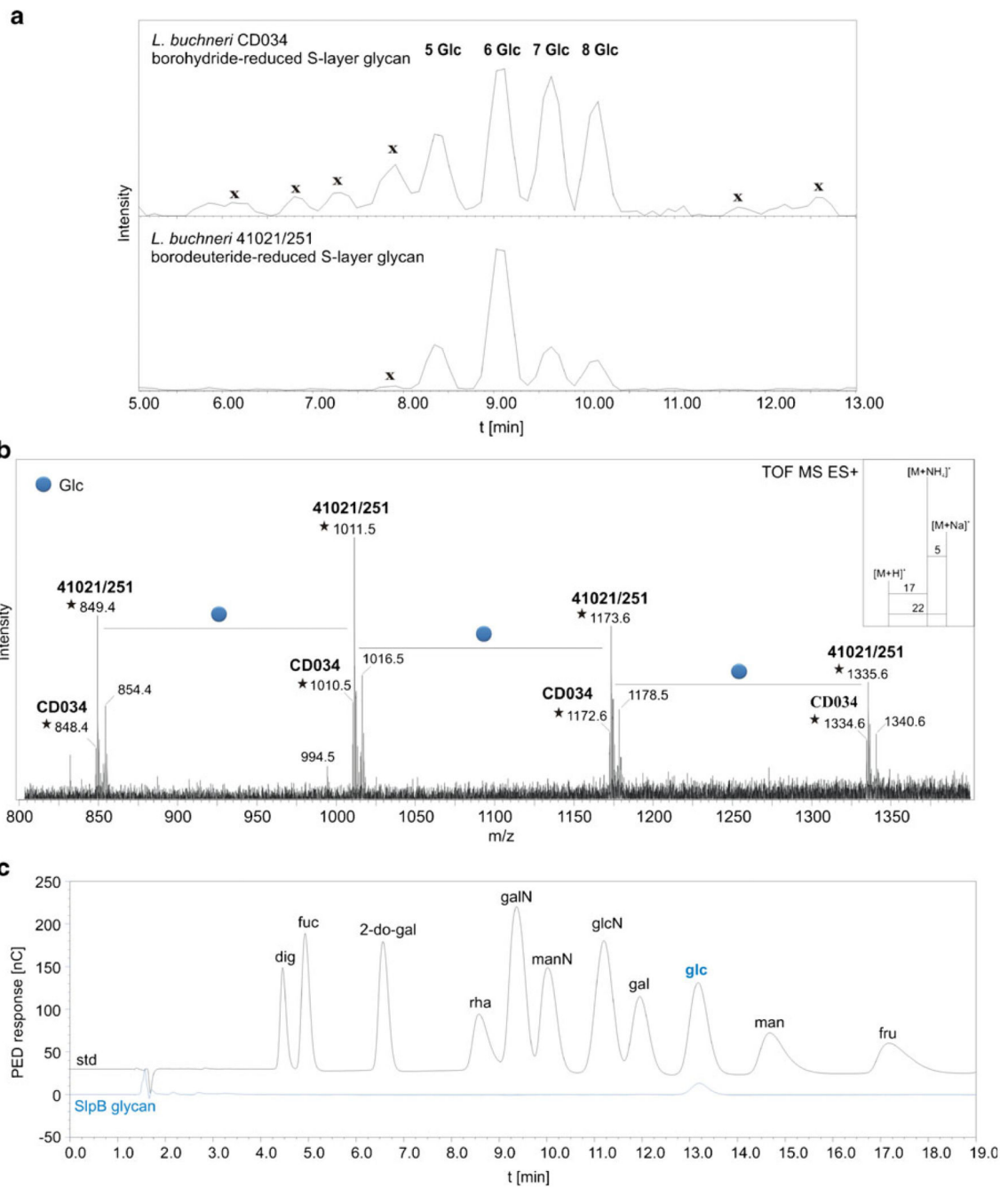
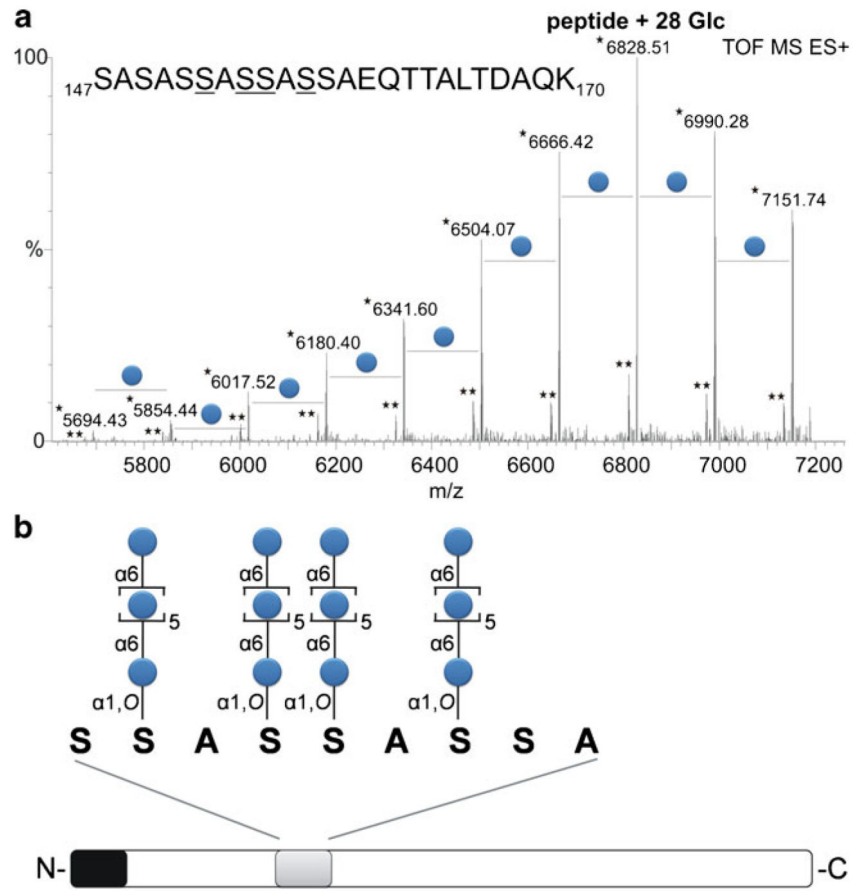


Fig. 3. Comparison of S-layer glycan profiles of *L. buchneri* CD034 and *L. buchneri* 41021/251. Glycans were released from the protein backbone *via* reductive β -elimination using NaBH_4 and NaBD_4 for *L. buchneri* strain CD034 and strain 41021/251, respectively. **a** LC profiles showing identical elution times of both glycans. Sample impurities are indicated with x. **b** Deconvoluted ESI-TOF-MS spectrum of released S-layer glycans from both strains premixed in one single run. Due to the use of deuterium for reduction of the *L. buchneri* 41021/251 S-layer glycan, a mass difference of 1 Da compared to the ^1H -reduced glycan of

L. buchneri CD034 was observed. As shown in **(b)**, glycans from both strains could therefore be analyzed in one single measurement. Adducts are according to ammonium and sodium as depicted in the inset. Molecular ions indicated with an asterisk are $[M+NH_4]^+$. Peaks representing repeating glucose units were observed for both strains. **c** HPAEC-PED profile of SlpB glycan monosaccharides after TFA hydrolysis

**Fig. 4.**

a Mass distribution of the glycosylated peptide of the S-layer protein of *L. buchneri* CD034. After a tryptic digest the glycopeptide (amino acid sequence given in the figure) was applied to LC-ESI-MS. The m/z values correspond to the sum of the mass of the amino acids and the glucoses attached to the peptide. The major peak at an m/z value of 6828.51 refers to the mass of 28 glucoses distributed over the peptide, with a calculated m/z value of 6828.57. [M+H+2NH₃]⁺ ions and [M+NH₄]⁺ ions are indicated by an asterisk and a double asterisk, respectively. Derivatization of glycosylated serines *via* ammonia based non-reductive β-elimination and ESI-TOF-MS/MS analysis (Fig. 5) revealed the presence of four glycosylation sites (*underlined*). **b** Schematic drawing of the S-layer glycoprotein of *L. buchneri* CD034. Based on glycan, glycopeptide as well as protein analysis, the S-layer glycoprotein possesses a signal peptide (*black*) consisting of 31 amino acids and an O-glycan consisting of on average seven Glc(α1–6) units attached to four serines within the acceptor sequence motif S-S-A-S-S-A-S-S-A (*grey*), corresponding to positions Ser₁₅₂, Ser₁₅₄, Ser₁₅₅, and Ser₁₅₇

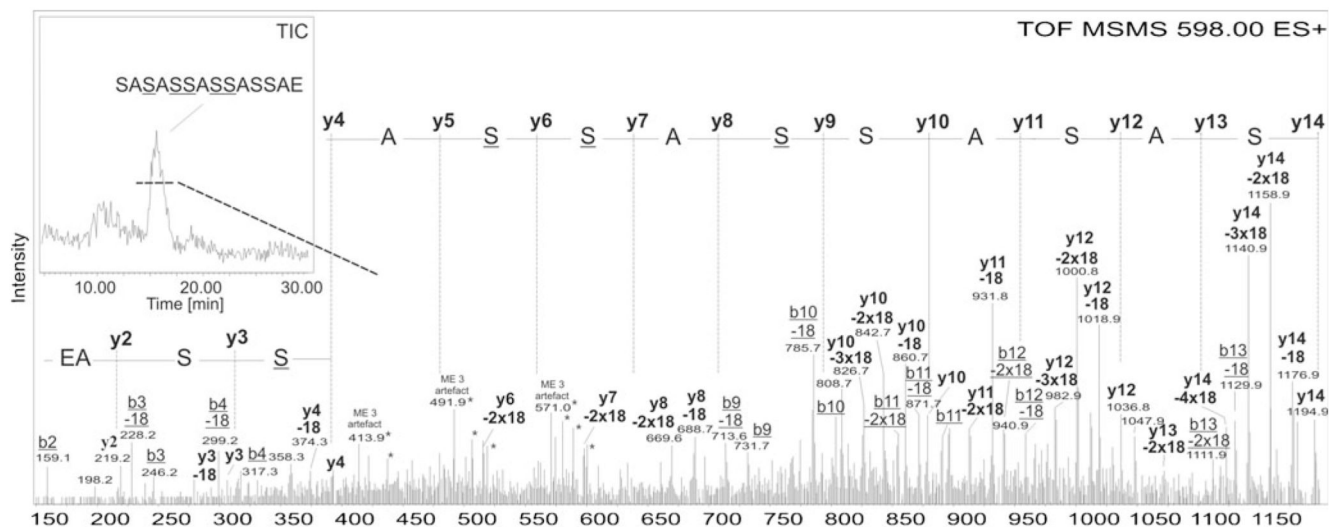


Fig. 5.

Mass spectrometric determination of the *O*-glycosylation sites on the S-layer protein of *L. buchneri* CD034. The glycopeptide was subjected to RP-ESI-TOF-MS/MS after ammonia-based non-reductive β -elimination. As depicted in the inset, the deglycosylated peptide eluted at a high percentage of acetonitrile (>30 %) as a broad peak. Mainly the B- and Y-series ions were found in the MS/MS spectrum. All ions in the spectrum, if not indicated otherwise, are $[M+H]^+$. Loss of 18 Da was detected for each peak originating from the Ser residues, most probably, due to loss of OH-groups. Deglycosylated Ser was found with 86 Da (-1 Da)

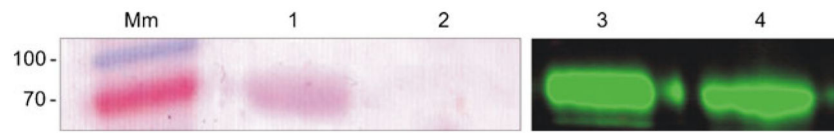


Fig. 6.

Cellular localization of protein glycosylation and in *L. buchneri* CD034. *L. buchneri* proteins were isolated from the cell wall (lanes 1 and 3) and the cytosolic fraction (lanes 2 and 4) of *L. buchneri* CD034 as described in Materials and Methods. Samples were run on SDS-PAGE (15 % gel), PAS-stained for carbohydrates (lanes 1 and 2) and Western-blotted and detected with S-layer specific antiserum (lanes 3 and 4). Mm, PageRuler prestained protein ladder (Thermo Scientific)

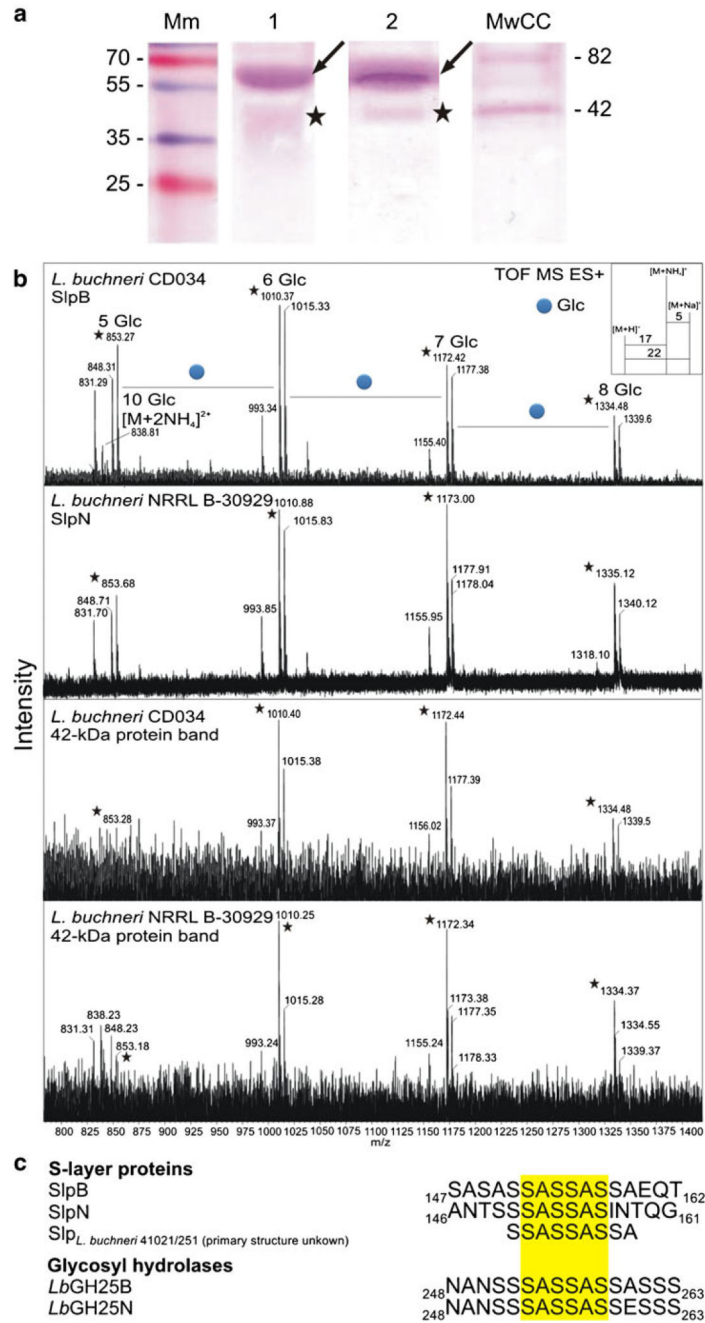


Fig. 7. Comparative analysis of protein glycosylation in *L. buchneri* strains. **a** Crude extracts of *L. buchneri* CD034 (lane 1) and *L. buchneri* NRRL B-30929 (lane 2) were run on SDS-PAGE (20 % gels) and PAS-stained for carbohydrates. The arrow and the asterisk indicate the S-layer proteins and the 42-kDa glyco-positive band, respectively. Mm, PageRuler Plus prestained protein ladder (Thermo Scientific); MmCC, Candy Cane Glycoprotein Molecular Weight Standards (Life Technologies). **b** Deconvoluted ESI-TOF-MS spectra of glycans released from *L. buchneri* CD034 and NRRL B-30929 glycoprotein bands after in-gel β -

elimination in comparison with *O*-glycans of the S-layer protein SlpB of *L. buchneri* CD034. *O*-glycans from all proteins were found to be identical. Molecular ions indicated with an asterisk are $[M+NH_4]^+$. **c** Confirmed (SlpB) and predicted glycosylation sites of *O*-glycans in *L. buchneri* strains. The common sequence motif S-A-S-S-A-S (yellow background) was found in all investigated proteins

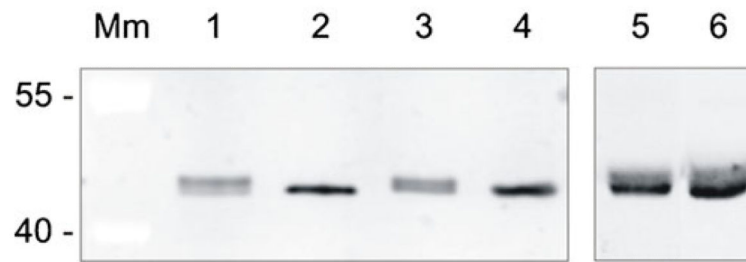


Fig. 8.

Apparent mass differences between native and recombinant glycosyl-hydrolases. *L. buchneri* CD034 and NRRL B-30929 cell extracts (lanes 1 and 3), recombinant *LbGH25B* and *LbGH25N* (lanes 2 and 4), premixed *L. buchneri* CD034 cell extract and recombinant *LbGH25B* (lane 5) and premixed *L. buchneri* NRRL B-30929 and recombinant *LbGH25N* were run on SDS-PAGE (9 % gel), Western-blotted and detected with glycosyl-hydrolase specific antiserum. Mm, PageRuler prestained protein ladder (Thermo Scientific)

Table 1

MS/MS peak identification and *O*-glycosylation site determination. Red colored masses were detected after the MS/MS experiment of the deglycosylated peptide. The series of minus 18 Da originates, most probably, from the loss of the serine OH groups. Glycosylation sites, indicated in bold, were found with 86Da. Mass deviation was found to be -0.5 Da for larger masses

mi	AA	loss of 18			B series	Y series	loss of 18		
87	S	34.0	52.0	70.0	88	1195.5	1177.5	1159.5	1141.5
71	A	105.1	123.1	141.1	159.1	1108.5	1090.5	1072.5	1054.5
87	S	192.1	210.1	228.1	246.1	1037.4	1019.4	1001.5	983.4
71	A	263.1	281.1	299.1	317.1	950.4	932.4	914.4	896.4
87	S	350.2	368.2	386.2	404.2	879.4	861.4	843.4	825.4
86	S	436.2	454.2	472.2	490.2	792.3	774.3	756.3	738.3
71	A	507.2	525.2	543.2	561.2	706.3	688.3	670.3	652.3
86	S	593.3	611.3	629.3	647.3	635.3	617.3	599.3	581.3
86	S	679.3	697.3	715.3	733.3	549.2	531.2	513.2	495.2
71	A	750.3	768.3	786.3	804.3	463.2	445.2	427.2	409.2
86	S	836.4	854.4	872.4	890.4	392.2	374.2	356.2	338.2
87	S	923.4	941.4	959.4	977.4	306.1	288.1	270.1	252.1
71	A	994.4	1012.4	1030.4	1048.4	219.1	201.1	183.1	165.1
129	E	1123.5	1141.5	1159.5	1177.5	148.1	130.1	112.1	94.1